Evaluation of Characteristics and Turn-off dV/dt Controllability of 1.2 kV SiC Si Hybrid Power Switch

Alireza Sheikhan and E. M. Sankara Narayanan
Department of Electronic and Electrical Engineering
The University of Sheffield.
Sheffield, United Kingdom

Abstract

Maintaining high efficiency and low power loss during different load conditions are key requirements for power electronic applications including electrical motor drives. Silicon carbide (SiC) MOSFETs offer fast switching with low losses. However, the cost of SiC MOSFETs is significantly higher compared to silicon (Si) trench IGBTs and will remain so for a considerable future. Also, at high currents, the on-state resistance of SiC MOSFETs becomes higher compared to the slope resistance of Si trench IGBTs. Furthermore, the sharp switching edges of SiC MOSFETs and their high dV/dt can cause degradation of motor winding or failure, detrimental bearing current and electromagnetic interference (EMI). This paper reports the device characteristics, working principle, and dV/dt controllability during turn-off of a 1200V hybrid power switch (HPS) based on parallel configuration of Si IGBT and SiC MOSFET technologies. The results, which are based on the latest IGBT and SiC technologies, show a significant reduction in switching as well as conduction losses and show that such a combination can combine the advantages of both of these technologies while being cost effective. It is demonstrated that the hybrid power switch can achieve switching losses as low as a SiC MOSFET with intelligent control of the device.

Keywords: Silicon Carbide, MOSFET, IGBT, Hybrid Power Switch, Power Density

INTRODUCTION

Silicon based insulated gate bipolar transistors (IGBTs) are key players in industrial motor drives and electric vehicle (EV) traction systems because of their high performance to cost ratio. IGBTs rely on conductivity modulation schemes where both electrons and holes contribute to the current flow to achieve a lower on-state resistance beyond the 1-dimensional material limit of silicon. While this is beneficial for on-state resistance, this feature also limits the switching speed, particularly during turn-off. The additional charges created by the conductivity modulation need to be evacuated from the drift region before the device can turn-off. The charge removal process is slow due to a long carrier lifetime which results in a tail current effect that increases the switching losses. IGBTs also suffer from an inherent p-n junction voltage drop of ~0.7V that results in significant conduction losses at low current levels. Moreover, trench IGBTs suffer from dynamic avalanche. Dynamic avalanche appears during turn-off switching transitions where the current filamentation may occur near trench gate edges at high dV/dt conditions [1]. This poses a fundamental current limiting factor for IGBTs to achieve high power density, low switching losses and long-term reliability [2, 3]. Unipolar devices such as SiC MOSFETs, are capable of fast switching with low losses that are at least an order of magnitude lower than their silicon IGBT counterparts [4, 5]. Unlike IGBTs, they turn-on at zero drain bias as long as the applied gate voltage is above its threshold voltage that enables current flow with low on-state resistance particularly at low current levels. However, a major issue is the significantly high costs related to these devices. The costs increase significantly with area (or current) requirements due to defect density limitations and associated yield.

In EVs, the power is sourced from battery packs or fuel cells which have a limited capacity. Thus, high efficiency is a critical aspect in the design of electrical powertrain to sustain over a distance. Since such systems operate at wide ranging load conditions, power semiconductor devices should be capable of sustaining efficient low loss operation over a wide range. It is clear that neither of these technologies (Si IGBTs or SiC MOSFETs) can offer a complete solution today. This is one of the reasons why most, if not all the EV drive systems include parallel combinations of SiC MOSFETs and Si IGBTs as separate modules.

Hybrid power switches (HPS) have been proposed to combine the advantages of bipolar and unipolar devices [6, 7]. HPS are formed by parallel configuration of IGBTs and MOSFETs. The exact ratio of MOSFET to IGBT depends on the application requirements and their mission profiles. Many studies have reported HPS designs based on discrete packaged devices and recently in module formats [8-16]. HPS current and power rating can be scaled up by addition of more Si IGBTs without a significant increase in costs and switching losses. Hybrid devices rely on a MOSFET (or multiple MOSFETs) for

handling partial load current conditions as well as switching transitions. IGBTs, have longer switching delay times than MOSFETs. The gate drive circuitry is one of the main challenges in HPS designs. A special gate drive circuit scheme is needed to account for the delay times of each individual switch in such a way to ensure the MOSFET is turned-off after the IGBT. Several studies have reported various gate driver designs for HPS [17, 18].

One of the key aspects of hybrid switches for their application into industrial motor drives and EVs is their dV/dt controllability. In motor drives, a high dV/dt can induce a detrimental bearing current, insulation degradation or failure of motor windings that limits the operational life span of the system [19-21]. Also, a high slew-rate contributes to EMI related issues if not controlled. To address these challenges, addition of passive filter components is necessary which results in increased weight, size, and costs [22]. Alternatively, this requirement can be met through dV/dt control of the power switching devices which can be realised via a high gate resistor which results in higher switching losses.

This paper presents a hybrid device configuration based on discrete Si IGBT [23] and SiC MOSFET [24] both of which are housed in TO-247 package. The device characteristics, working principle and turn-off dV/dt controllability are presented and analysed. The turn-off energy loss is also investigated with respect to the dV/dt to evaluate the improvements against the HPS constituent components, IGBT and MOSFET.

DEVICE STRUCTURE & CHARACTERISTICS

Configuration and Working Mechanism

The hybrid device is made by parallel configuration of a SiC MOSFET (CoolSiC from Infineon) [24] and Si IGBT (IGBT7 from Infineon) [23] as shown in Fig. 1. Both devices are rated 50A and 1200V and are housed in TO-247 packages.

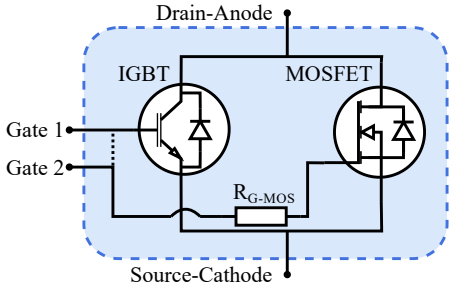

Fig. 1. 1200V hybrid power switch (HPS) configuration. The gates can be controlled independently or connected depending on the gate driver configuration.

The MOSFET is much faster, and its delay time is smaller than the IGBT. Consequently, during the turn-on, the MOSFET is switched prior to the IGBT. Thus, the turn-on behaviour is mainly determined by the MOSFET. However, during the turn-off, this leads to undesirable turn-off of the MOSFET before IGBT. Ideally the two gates need to be controlled independently to ensure that the IGBT is turned-off before the MOSFET. Alternatively, this can partially be improved by adding a separate gate resistor ($R_{G\text{-}MOS}$) for the MOSFET. The resistor increases the delay time of the MOSFET. The drawback of this method is that it limits the slew-rates of the device. The resistor can also help to dampen high frequency gate oscillations due to parasitic inductances and characteristics mismatch. The constituent components of the HPS are capable of withstanding short circuit fault. The IGBT and MOSFET are rated for short circuit withstand time of 8µs at 600V and 3µs at 800V respectively [23, 24].

In forward conduction mode, the device operates in unipolar or bipolar regime depending on the load current. At high load current of above ~35A, the IGBT handles the majority of current due to its lower resistance. Meanwhile, at low current levels, the current is primarily handled by the MOSFET. The exact current sharing between the individual devices depends on the on-state resistance and voltage drop of each device at a given operating current and temperature. The reverse conduction is facilitated via the IGBT extrinsic Si diode and the MOSFET. An ideal solution would be to co-pack a SiC Schottky barrier diode that has a low reverse recovery and fast switching characteristics. In this paper, the HPS performance is tested with both gates connected using a single gate control and separately using dual gate control.

Forward Characteristics and On-state Behaviour

The forward I-V characteristics of the hybrid device were measured at room temperature at different gate voltages as shown in Fig. 2.

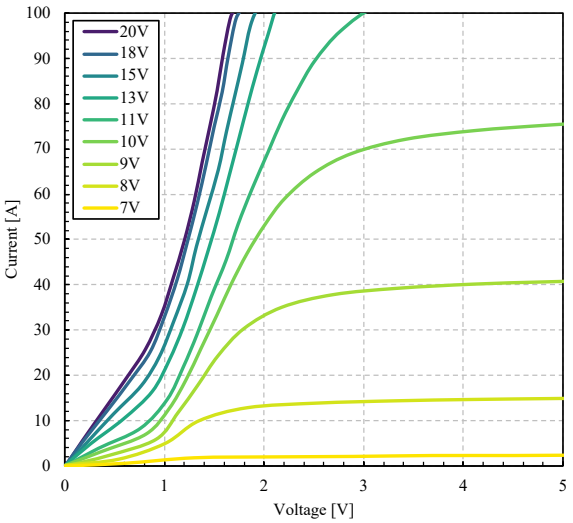

Fig. 2. Measured forward (I-V) characteristics of the hybrid power switch at different gate voltages at 25˚C. The pulse width is 250µs.

The voltage drop across the device is 1.2V at 50A, 18V gate voltage, and at 25˚C. This is 28% and 39% lower than the individual components of IGBT and MOSFET

respectively. The I-V curves of the hybrid device are compared to constituent individual devices as shown in Fig. 3.

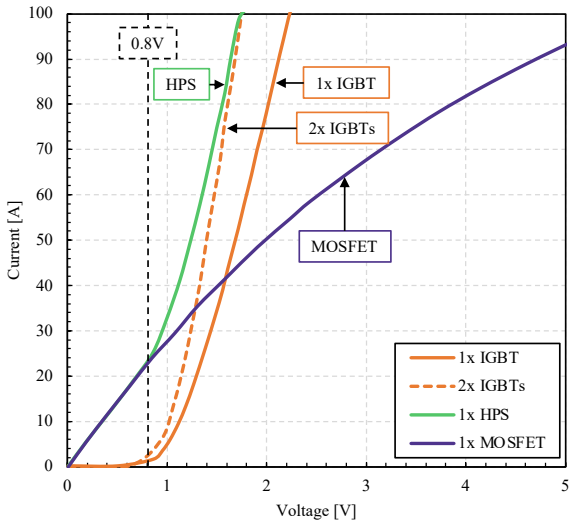

Fig. 3. Measured I-V curves of devices at 25˚C. The gate voltage is 18V.

In the low current region of less than 25 A, the HPS characteristics match with the 1x MOSFET. This is because the voltage across the IGBT must be higher than ~0.7V before it can conduct any current at room temperature. On the other hand, due to the unipolar nature of the MOSFET, there is no initial voltage drop and the device conducts at any drain voltage (V_{ds}) larger than 0V when the gate voltage (V_{gs}) is higher than its threshold voltage ($V_{gs\text{-}th}$). In high current region, above 25A, the HPS enters the bipolar mode of operation. The MOSFET resistance rises and the current starts to divert to the IGBT. This characteristic of the HPS can result in an optimum current handling capability over a wide range of load conditions. To evaluate the conduction losses, the on-state voltage drops of the HPS, and each individual component are measured at 50A at different junction temperatures as illustrated in Fig. 4.

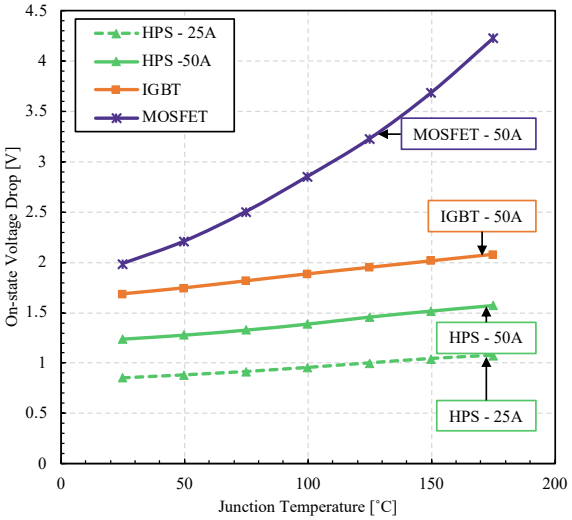

Fig. 4. Measured comparison of the on-state voltage drops of the HPS and its individual components at different junction temperatures at gate voltage of 18V.

SiC MOSFETs have a higher positive temperature coefficient of voltage than the Si IGBT and the HPS. This is because of the conductivity modulation of the IGBT and HPS. Therefore, the HPS can maintain a minimal conduction loss over a wide range of load current and temperatures. At high operating temperatures (175˚C), the hybrid device shows 63% lower voltage drop compared with that of the MOSFET. It is also important to note that as the temperature rises, the bipolar onset voltage decreases and IGBTs can conduct at lower drain/anode voltages. This property enables the HPS to demonstrate high efficiency at high temperatures.

Reverse Conduction Characteristics

The reverse conduction characteristics of the HPS are shown in Fig. 5 and compared with the HPS components.

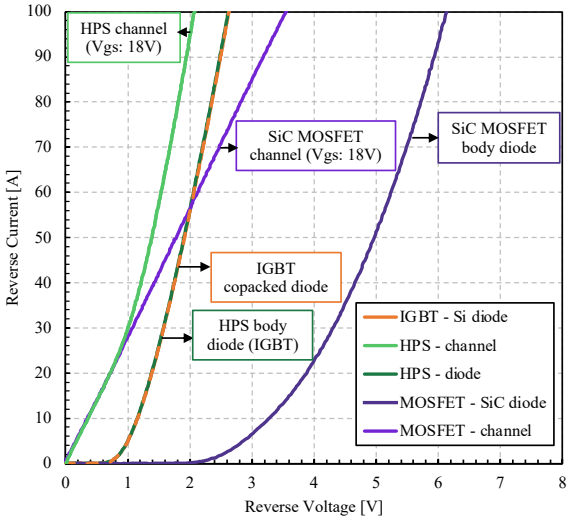

Fig. 5. Measured reverse characteristics of the HPS and its integral components.

The HPS consists of an IGBT that is co-packed with an extrinsic Si diode and a SiC MOSFET that has an intrinsic SiC body diode. The SiC p-n body diode has a high forward voltage drop of 5V at 50A while the forward voltage drop of Si diode at 50A is 1.9V. During the off-state (V_{gs} = 0V), the reverse characteristic of the HPS is identical to the IGBT co-packed Si diode. Once a positive gate voltage (V_{gs} = 18V) is applied, the voltage drop decreases further as the current is shared between the MOSFET and the co-packed Si diode. The voltage drop of the HPS during reverse conduction is 1.39V compared with 1.78V of the MOSFET at 50A because the current is shared by the Si diode within the HPS. Under normal operating conditions, the SiC body diode does not contribute to current flow due to its high forward voltage drop.

EXPERIMENTAL SETUP

A clamped inductive switching test bench was set up to evaluate the switching performance of the hybrid power switch as shown in Fig. 6.

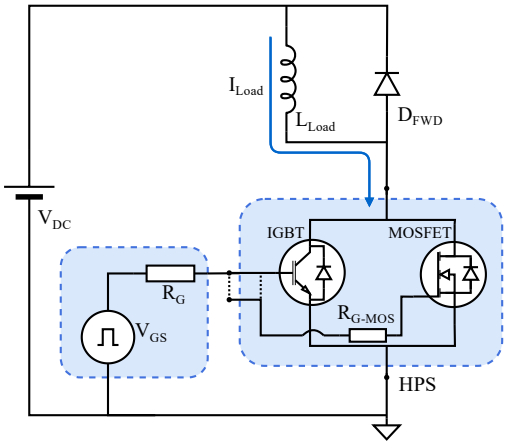

Fig. 6. Simplified circuit diagram of the experimental setup.

The setup uses a 240µH inductor as the load which is clamped by a 1200V SiC Schottky barrier diode (D_{FDW}). The supply voltage (V_{DC}) is fixed at 600V, and the load current (I_{load}) is 50A. The test was conducted at different external gate resistor values to determine the dV/dt controllability and switching losses. In part one of the experiment, the HPS was controlled using a single gate drive approach. In this configuration both gates are connected. The gate drive circuitry provides a pulse with an amplitude of +18V and -5V for turn-on and turn-off respectively. In the second part, a dual gate control was implemented to control the HPS gates separately. In this part, the turn-off gate voltage is 0V and -5V for the MOSFET and IGBT respectively. The positive gate voltage is 18V for both devices. A delay time of ~1µs is imposed on the MOSFET. The experiment was repeated for individual components of the hybrid device for comparison purposes. For fair evaluation, the gate driving conditions are kept the same. The dV/dt and rise time are calculated based on the changes in drain/anode voltage from 10% to 90% of the drain switching transition. The switching power losses are determined by the overlap of the voltage and current during the switching transition and it is then integrated to calculate the energy loss.

MEASUREMENTS RESULTS AND DISCUSSION

Independent Gate Control Method

As previously mentioned, MOSFETs delay times are generally shorter than their IGBTs counterparts which is particularly important during the turn-off. To address this issue, two gate signals are required to add a delay to the MOSFET gate. This results in a smaller pulse width applied to the IGBT gate. Fig. 7 shows the dual gate control waveforms of the HPS.

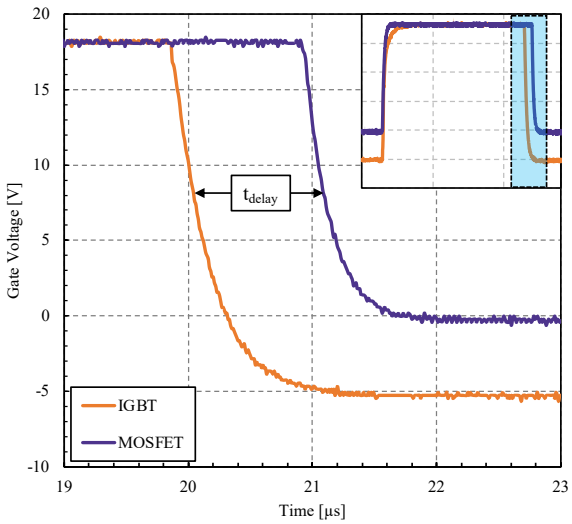

Fig. 7. Measured Individual gate of the HPS using independent dual gate control.

The delay time needs to be adjusted to ensure that the IGBT is fully switched-off before the MOSFET. The switching waveforms of the HPS with ~1µs delay time is shown in Fig. 8.

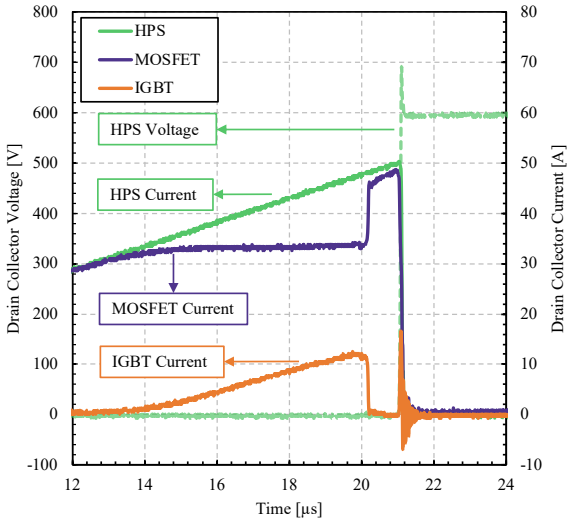

Fig. 8. Measured turn-off switching waveforms of the HPS using dual gate control.

In this configuration, the IGBT experiences zero-voltage-switching (ZVS) and does not contribute to the switching losses of the HPS. Consequently, the switching characteristics of the HPS is mainly determined by its MOSFET. As the HPS current rises, the MOSFET drain current is clamped to ~34A, as the IGBT takes over current share due to its lower voltage drop. As the IGBT turns-off, the current is diverted to the MOSFET for the period of delay time that causes a surge current. The delay time should be kept minimal to avoid extra load stress on the MOSFET.

Turn-Off Switching Characteristics

The test was conducted to determine and evaluate the turn-off switching characteristics and dV/dt controllability of the hybrid power switch. Initially, the HPS was tested with a single gate control. The corresponding switching waveforms are shown in Fig. 9 at different gate resistances.

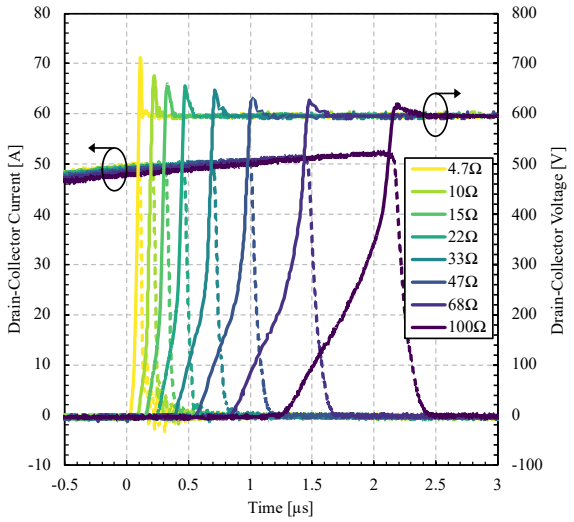

Fig. 9. Measured turn-off switching waveforms of the HPS using the single gate control at different gate resistances. The gate voltage is 18V and -5V for turn-on and turn-off respectively.

The test was repeated for the HPS using dual gate control approach. In this configuration both gates were driven independently. A delay time of 1µs was added to ensure the IGBT turns off before the MOSFET. The gate resistor for the IGBT was fixed at 15Ω and the gate resistor for the MOSFET was varied from 1Ω to 150Ω. The turn-on and turn-off gate voltage is 18V and 0V for the MOSFET respectively. The turn-on gate voltage of the IGBT is also 18V with -5V for the turn-off. The corresponding switching waveforms are shown in Fig. 10.

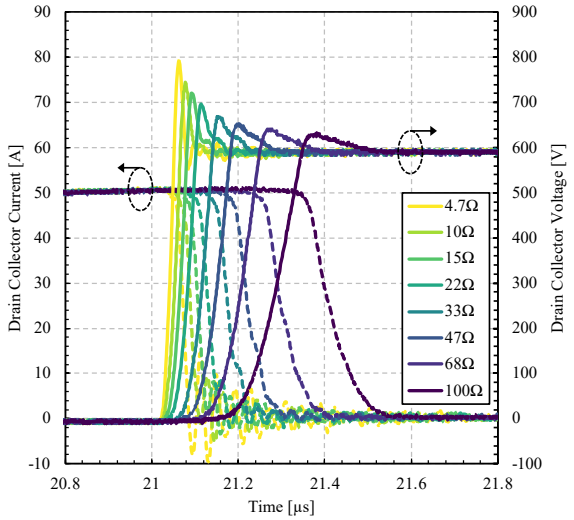

Fig. 10. Measured turn-off switching waveforms of the HPS using dual gate control at different gate resistances. The IGBT gate resistance is fixed at 15Ω with a 1µs delay time.

In both configurations, the switching slew-rates decrease as the gate resistor value increases, which demonstrates the dV/dt controllability of the hybrid device. It can be observed that at high gate resistances the switching waveforms of the HPS using a single gate control are like the IGBT switching waveforms shown in Fig. 11. This is because the delay time of the IGBT is dominant at high gate resistances.

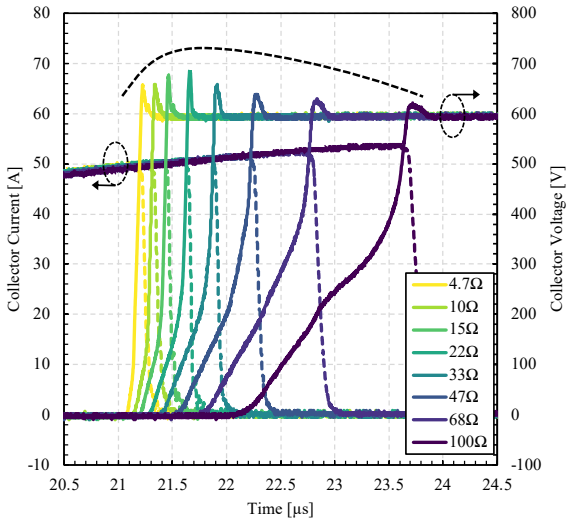

Fig. 11. Measured turn-off switching waveforms of two IGBTs in parallel configuration at different gate resistances. The gate voltage is 18V and -5V for turn-on and turn-off respectively.

While the slew rate slows down at high gate resistances, an inverted 'U' shape can be seen by the peaks which is attributed to dynamic avalanche. This is a critical limitation for IGBTs which limits their operating dV/dt. For example, in this case, the device's minimum required gate resistor for reliable operation is about 22Ω to effectively suppress the dynamic avalanche. In hybrid configurations, dynamic avalanche is suppressed because the current is handled by the MOSFET which does not suffer from dynamic avalanche.

dV/dt Controllability and Switching Losses

The dV/dt and voltage rise time of the HPS were extracted from the measured switching waveforms and compared with the HPS constituent components as shown in Fig. 12.

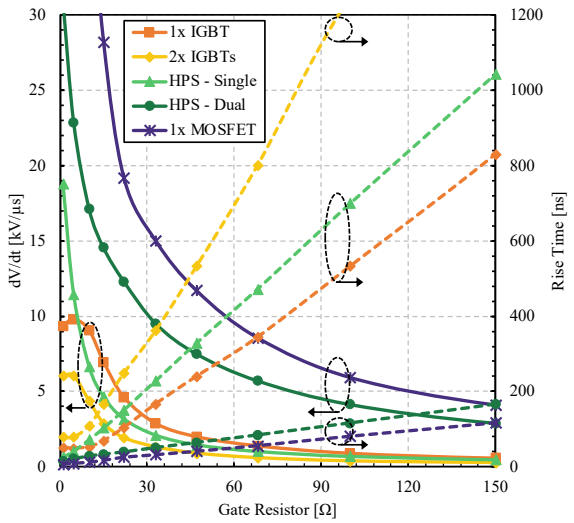

Fig. 12. Measured dV/dt and rise time of the HPS and its components. HPS single refers to the single gate drive and HPS dual refers to the dual gate drive methods.

Due to the absence of dynamic avalanche in the HPS, dV/dt can reach as high as 19kV/µs with single gate control. The HPS dV/dt can further increase beyond 30kV/µs by using a separate dual gate control. The dV/dt of the 1x IGBT and 2x IGBTs are limited due to presences of dynamic avalanche at low gate resistances (R_g < 10Ω). In the dual gate approach of the HPS, the IGBT turn-off transition is completed before the MOSFET, and the gate capacitances are discharged. The output capacitance of the IGBT and its co-packed diode, however, needs to be charged and thus the rise time is slightly higher than the 1x MOSFET.

The corresponding turn-off energy losses are calculated from the measured data for each device as shown in Fig. 13.

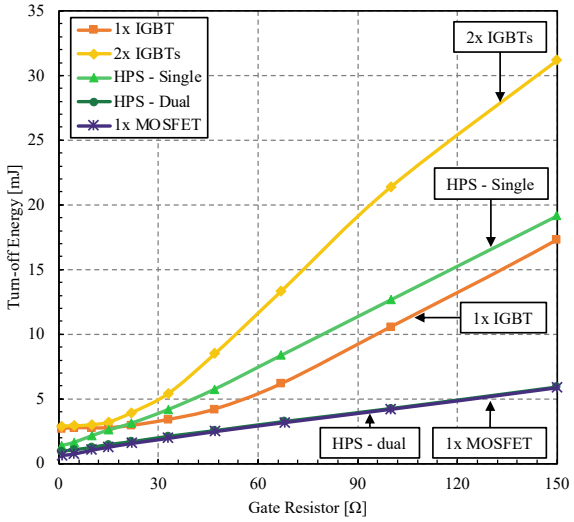

Fig. 13. Comparison of the corresponding turn-off switching energy losses at different external gate resistances.

The HPS using a dual gate control offers a significant reduction in energy losses due to the enhanced switching capability. In this configuration the IGBT is not involved in the switching and the MOSFET determines the switching behaviour. Therefore, the turn-off energy of the HPS using dual gate control is effectively the same as 1x MOSFET. Also, with a single gate control, the HPS switching losses are much lower compared to the equivalent 2x IGBTs. It is important to note that, in both 1x IGBT and 2x IGBTs, the energy losses are not linear at lower gate resistances (R_g < 22Ω) because of the dynamic avalanche. As stated before, such an effect does not exist in the HPS configuration.

CONCLUSION

In this work, a hybrid device configuration using a Si IGBT and a SiC MOSFET is presented. The device characteristics, working mechanism and turn-off dV/dt controllability are demonstrated experimentally. It has been shown that the hybrid device can combine the advantages of both technologies in terms of cost and performance effectively while maintaining a low power loss under different load conditions. The device can operate in unipolar or bipolar mode depending upon the current level. The hybrid configuration also maintains a low conduction loss at high operating temperatures. The switching losses show a significant reduction compared to its constituent components as standalone devices. With independent gate control of the HPS, the switching losses can be further optimised. Choosing the appropriate MOSFET is essential as the current during partial load is significantly affected by it. The concept can be scaled up according to the application requirements to accommodate a larger current capacity by addition of more IGBTs. The optimum ratio of IGBT to MOSFET can be investigated in future works. Overall, the hybrid device concept offers a significant reduction in cost to performance ratio due to the widely accessible low price of Si devices, which well suits integration in intelligent power modules.

REFERENCES

[1] J. Lutz and R. Baburske, “Dynamic avalanche in bipolar power devices,” *Microelectronics Reliability,* vol. 52, no. 3, pp. 475-481, 2012.

[2] S. Machida, K. Ito and Y. Yamashita, “Approaching the Limit of Switching Loss Reduction in Si-IGBTs,” in *International Symposium on Power Semiconductor Devices & IC's (ISPSD)*, Waikoloa, 2014.

[3] T. Ogura, H. Ninomiya, K. Sugiyama and T. Inoue, “Turn-off switching analysis considering dynamic avalanche effect for low turn-off loss high-voltage IGBTs,” *Transactions on Electron Devices,* vol. 51, no. 4, pp. 629 - 635, 2004.

[4] M. Rahimo, “Performance Evaluation and Expected Challenges of Silicon Carbide Power MOSFETs for High Voltage Applications,” *Materials Science Forum,* vol. 897, pp. 649-654, May 2017.

[5] A. Sheikhan, E. M. S. Narayanan, H. Kawai, S. Yagi and H. Narui, "Evaluation of turn-off dV/dt controllability and switching characteristics of 1.2kV GaN polarisation superjunction HFETs," *Japanese Journal of Applied Physics,* vol. 62, p. 064502, 2023.

[6] D. Y. Chen and S. A. Chin, "Bipolar-FET Combinational Power Transistors for Power Conversion Applications," in *Fifth International Telecommunications Energy Conference*, Tokyo, 1983.

[7] Y. Jiang, G. Hua, E. Yang and F. Lee, "Soft-switching of IGBTs with the help of MOSFETs in bridge-type converters," in *IEEE Power Electronics Specialist Conference*, Seattle, 1993.

[8] A. Deshpande, R. Paul, A. I. Emon, Z. Yuan, H. Peng and F. Luo, "Si-IGBT and SiC-MOSFET hybrid switch-based 1.7 kV half-bridge power module," *Power Electronic Devices and Components,* vol. 3, p. 100020, 2022.

[9] P. Luo, H. Y. Long, M. R. Sweet, M. M. D. Souza and E. M. S. Narayanan, "Analysis of a Clustered IGBT and Silicon Carbide MOSFET Hybrid Switch," in *26th International Symposium on Industrial Electronics (ISIE)*, Edinburgh, 2017.

[10] R. A. Minamisawa, U. Vemulapati, A. Mihaila, C. Papadopoulos and M. Rahimo, "Current Sharing Behavior in Si IGBT and SiC MOSFET Cross-Switch Hybrid," *Electron Device Letters,* vol. 37, no. 9, pp. 1178 - 1180, 2016.

[11] A. Deshpande and F. Luo, "Practical Design Considerations for a Si IGBT + SiC MOSFET Hybrid Switch: Parasitic Interconnect Influences, Cost, and Current Ratio Optimization," *IEEE Transactions on Power Electronics,* vol. 34, no. 1, pp. 724 - 737, 2019.

[12] G. Ortiz, C. Gammeter, J. W. Kolar and O. Apeldoorn, "Mixed MOSFET-IGBT bridge for high-efficient Medium-Frequency Dual-Active-Bridge converter in Solid State Transformers," in *Workshop on Control and Modeling for Power Electronics (COMPEL)*, Salt Lake City, 2013.

[13] X. Song, A. Q. Huang, M.-C. Lee and C. Peng, "High voltage Si/SiC hybrid switch: An ideal next step for SiC," in *International Symposium on Power Semiconductor Devices & IC's (ISPSD)*, Hong Kong, 2015.

[14] H. Qin, D. Wang, Y. Zhang, D. Fu and C. Zhao, "Characteristics and Switching Patterns of Si/SiC Hybrid Switch," in *PCIM Asia 2017*, Shanghai, 2017.

[15] K. Hoffmann and J. Karst, "High frequency power switch - improved performance by MOSFETs and IGBTs connected in parallel," in *European Conference on Power Electronics and Applications*, Dresden, 2005.

[16] M. Rahimo, F. Canales, R. A. Minamisawa, C. Papadopoulos, U. Vemulapati, A. Mihaila, S. Kicin and U. Drofenik, "Characterization of a Silicon IGBT and Silicon Carbide MOSFET Cross-Switch Hybrid," *IEEE Transactions on Power Electronics,* vol. 30, no. 9, pp. 4638 - 4642, 2015.

[17] J. Wang, Z. Li, X. Jiang, C. Zeng and Z. J. Shen, "Gate Control Optimization of Si/SiC Hybrid Switch for Junction Temperature Balance and Power Loss Reduction," *IEEE Transactions on Power Electronics,* vol. 34, no. 2, pp. 1744 - 1754, 2019.

[18] Z. Li, X. Dia, X. Jiang, F. Qi, Y. Liu, P. Ke, Y. Wang and J. Wang, "A novel gate driver for Si/SiC hybrid switch for multi-objective optimization," *IET Power Electronics,* vol. 14, no. 2, pp. 422-431, 2021.

[19] E. Persson, "Transient effects in application of PWM inverters to induction motors," *IEEE Transactions on Industry Applications,* vol. 28, no. 5, pp. 1095-1101, 1992.

[20] A. V. Jouanne and P. Enjeti, "Design considerations for an inverter output filter to mitigate the effects of long motor leads in ASD applications," *IEEE Transactions on Industry Applications,* vol. 33, no. 5, pp. 1138-1145, 1997.

[21] A. V. Jouanne, P. Enjeti and W. Gray, "Application issues for PWM adjustable speed AC motor drives," *IEEE Industry Applications Magazine,* vol. 2, no. 5, pp. 10-18, 1996.

[22] H. Akagi, "Influence of high dv/dt switching on a motor drive system: a practical solution to EMI issues," in *International Symposium on Power Semiconductor Devices and ICs (ISPSD)*, Kitakyushu, 2004.

[23] Infineon, "IKW50N120CS7 - datasheet," Infineon, 2021.

[24] Infineon, "IMW120R030M1H - datasheet," Infineon, 2020.

Addresses of the authors

Alireza Sheikhan, Department of Electronic and Electrical Engineering, The University of Sheffield, Western Bank, Sheffield, United Kingdom, asheikhan1@sheffield.ac.uk

E. M. Sankara Narayanan, Department of Electronic and Electrical Engineering, The University of Sheffield, Western Bank, Sheffield, United Kingdom, s.madathil@sheffield.ac.uk